



The hydrogen embrittlement behavior of ultra-high-strength boron steel with different prior austenite grain sizes

Yi Liu¹, Xianhong Han^{1,†}, Yi Yang² and Haibing Yuan²

¹*School of Materials Science and Engineering, Shanghai Jiao Tong University, Shanghai 200030, China*

²*JiangSu Sunway Precision Forging Co., Ltd, Yancheng 224100, China*

[†]*E-mail: hanxh@sjtu.edu.cn*

The hydrogen embrittlement (HE) of ultra-high-strength boron steel with different prior austenite grain (PAG) sizes was investigated. By adjusting soaking times and austenitizing temperatures, samples with varying PAG sizes were obtained. The PAG size and dislocation density of the samples were measured using electron backscatter diffraction technology. Hydrogen microprint technology was employed to further examine the impact of PAG size on the HE behavior. The sensitivity of HE decreased with the increasing of PAG size. It can be attributed to the combination of PAG size and dislocation density. The reduction in PAG size leads to higher dislocation density which increases the sensitivity of HE and facilitates the accumulation of hydrogen at the small PAG boundaries. This promotes local high hydrogen concentration, and ultimately resulting in the higher HE sensitivity.

Keywords: Ultra-high strength steel; Hydrogen embrittlement; PAG sizes; Hydrogen microprint technique.

1. Introduction

Hot-stamping steel possesses ultra-high strength, excellent formability, impact resistance, and lightweight advantages, making it widely used in automotive body structures like A-pillars and B-pillars. However, its widespread application faces a significant challenge, i.e., hydrogen embrittlement (HE) [1]. HE arises from hydrogen atoms introduced during production or service, causing sudden fractures and catastrophic failures. To address the issue of hydrogen embrittlement, it is feasible to tailor microstructure and design hydrogen trapping sites to limit the diffusion and accumulation of hydrogen in the matrix. Grain refinement can effectively increase grain boundary area, enhancing the density of hydrogen trapping sites and improving resistance to HE. However, Masoumi et al. [2] claimed that fine grains with higher grain boundary density show a higher HE sensitivity. Moreover, Latypova et al. [3] reported that larger equiaxed PAG sizes exhibit better resistance to HE in quenched martensitic steel. These contradictory conclusions may result from different secondary influencing factors caused by various grain size control methods or intrinsic material properties. For instance, steel treated with quenching and tempering has varying dislocation densities, leading to different degrees of HE sensitivity.

This work investigates the sole impact of PAG size on the HE resistance of ultra-high-strength hot stamping steels (B1500HS) by varying austenitizing conditions. The hydrogen

microprint technique (HMT) was used to visualize hydrogen diffusion and illustrate the impact of grain boundaries on HE sensitivity.

2. Experiments

The ultra-high strength steel (B1500HS) provided by Baosteel Co., Ltd., has a thickness of 1.4 mm. To produce samples with different PAG sizes, various austenitizing conditions were applied, followed by water quenching. The soaking time (ST) was varied at 920 °C for 3 min, 5 min, 8 min, and 10 min. The austenitizing temperature (AT) was adjusted to 920 °C, 970 °C, and 1020 °C, with a constant soaking time of 5 min.

The electrochemical hydrogen charging method was employed with a current of 0.001 A (0.521 mA/cm²) for 1 h. The electrolyte consisted of a 0.5 mol/L H₂SO₄ solution with 1 g/L thiourea. The slow strain rate tensile (SSRT) was carried on using a constant extension machine (Instron 2382) at a nominal strain rate of 10⁻⁴ s⁻¹. The gauge dimensions of tensile samples are 16 × 6 × 1.4 mm³. The sensitivity of HE is defined as the loss of tensile strength (σ) and elongation (δ), calculated using equations (1) and (2), respectively.

$$\sigma_{loss} = \frac{\sigma_{air} - \sigma_{hydrogen}}{\sigma_{air}} \quad (1)$$

$$\delta_{loss} = \frac{\delta_{air} - \delta_{hydrogen}}{\delta_{air}} \quad (2)$$

Here, the subscript of *air* and *hydrogen* refers to uncharged and hydrogen-charged conditions, respectively. More details about microstructure characterization can be acquired in our previous work [4].

3. Results and discussion

Figs. 1a-f show the band contrast of the martensite phase combined with the inverse pole figure of the prior austenite phase for samples with different austenitizing treatments, revealing the lath martensite structure and PAG size simultaneously. Obviously, the grain size of prior austenite is increasing with the ST and AT. Fig. 1g exhibit the frequency distribution histogram of the PAG sizes. Statistical results indicate that average PAG sizes of samples with 3 min, 5 min, 8 min, and 10 min are around 8.54 μ m, 13.05 μ m, 15.03 μ m, and 19.74 μ m, respectively. The average PAG size of the samples austenitizing at 920 °C, 970 °C, and 1020 °C is around 13.05 μ m, 25.44 μ m, and 31.39 μ m, respectively. It can be concluded that finer PAG grains predominate in samples with less ST and lower AT.

Figs. 2a and 2d, as well as Figs. 2b and 2d compare the tensile strength and elongation of hydrogen-charged and non-hydrogen charged samples under different austenitizing treatments. Figs. 2c and 2f reveal the HE sensitivity of samples with different STs and ATs, respectively. For the non-hydrogen charged samples, tensile strength slightly decreases with the increase of ST and AT, while elongation remains nearly unchanged.

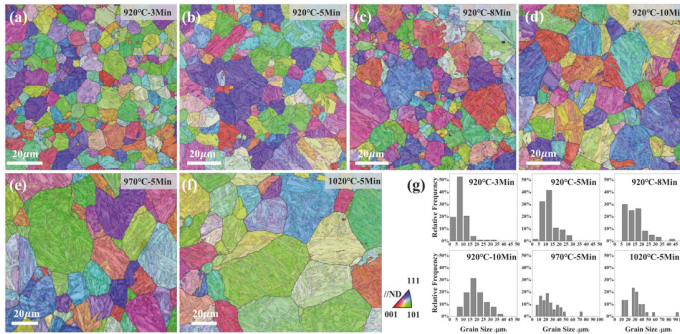


Fig. 1. (a-f) EBSD analysis of samples with different PAG sizes. (g) distribution of the PAG sizes.

After hydrogen charging, both tensile strength and elongation of all samples decrease to varying extents. Notably, compared to the moderate tensile strength loss, elongation shows a sharp loss. It can be found that both σ_{loss} and δ_{loss} decrease as ST and AT increases. Consequently, it can be inferred that samples subjected to increased ST and AT with larger PAG sizes are in favor of reduced HE sensitivity.

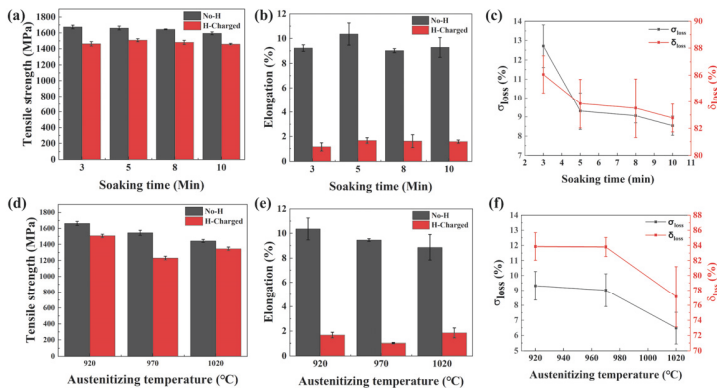


Fig. 2. (a, d) Tensile strength and (b, e) elongation of samples with different austenitizing treatments, respectively. (c, d) Statistics of σ_{loss} and δ_{loss} .

Fig. 3a illustrates the relationship between average PAG sizes and ST and AT. Apparently, the average PAG sizes increase with both ST and AT. The impact of grain size on HE sensitivity is attributed to its effect on hydrogen diffusion, explained through the interplay of two competing processes. Firstly, some research indicates that grain boundaries preferentially facilitate hydrogen diffusion, and refined grain size increases total hydrogen content but reduces it per unit area, thus lowering HE sensitivity. This is common in metals like austenitic steels and pure nickel, which typically show lower HE sensitivity. Secondly, in high HE sensitivity steels like martensitic steel, grain boundaries act as trapping sites that hinder hydrogen diffusion. As grain size is refined, more grain boundaries and triple junctions form, facilitating hydrogen accumulation, which reduces grain boundary cohesion and promotes intergranular fractures.

Additionally, dislocation, which is in a high density for as-quenched martensitic steel, significantly impact HE. With an increase in AT and ST, the geometrically necessary dislocation (GND) density, which is derived from EBSD data, shows a clear downtrend, contrary to the trend of the PAG sizes (Fig. 3a). In Fig. 3b, the higher GND density results in severe mechanical properties loss, i.e., the higher dislocation densities result in greater HE sensitivity.

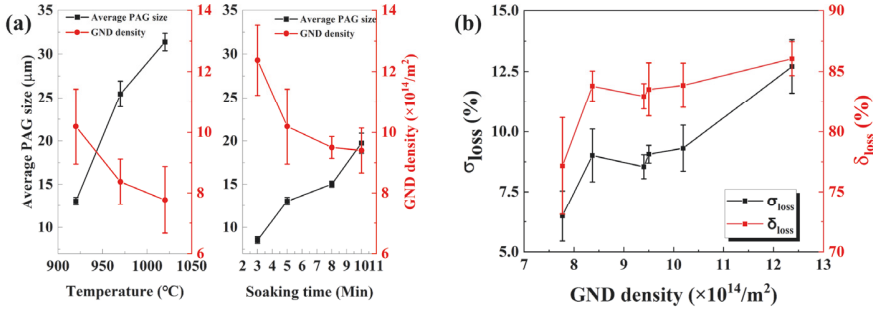


Fig. 3. (a) the average PAG size and GND density at different STs and ATs, (b) σ_{loss} and δ_{loss} at different GND densities.

The HE sensitivity of samples depends on hydrogen diffusion and distribution, influenced by the hydrogen introduction method. Electrochemical hydrogen charging leads to a high surface hydrogen concentration, resulting in a steep gradient near the charging surface. In the HMT experiment, as shown in Fig. 4, two regions are examined: near the hydrogen charging surface and the center of the thickness direction. In the central area, Ag particles (representing H atoms) are uniformly distributed within the martensitic matrix, considered hydrogen-trapping sites. At the edge, larger PAG size samples show no significant variation in Ag particle distribution, while finer PAG size samples exhibit non-uniform hydrogen distribution, with Ag particles located at PAG boundaries. Thus, hydrogen atom concentration slightly decreases from the surface inward in larger PAG size samples, and the hydrogen distribution near the surface is more uneven in fine PAG size samples. This difference is attributed to hydrogen introduction methods and requires further explanation for the heterogeneous distribution in fine PAG samples.

The impact of boundaries, effective hydrogen trapping sites, on hydrogen distribution in martensitic structures is significant. Small PAG sizes prevent the formation of multiple blocks or packets, reducing the hydrogen-trapping effect of multiple interfaces. This causes hydrogen atoms to accumulate at PAG boundaries. The high initial dislocation density in martensitic steel further promotes hydrogen aggregation at these boundaries. PAG boundaries have higher vacancy concentrations [5], and hydrogen atoms bind strongly to these vacancies, forming complexes that require high dissociation enthalpy to migrate [6]. Thus, hydrogen atoms are trapped at PAG boundaries, creating a high hydrogen barrier and local high hydrogen concentration near the charging surface. This high hydrogen concentration leads to premature crack formation under external loads, making samples with finer PAG sizes more HE sensitive.

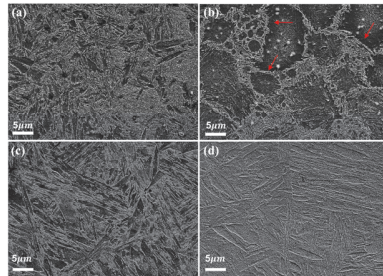


Fig. 4. SEM images of the hydrogen-charged samples after HMT treatment. (a-b) 920°C-3min, (d-e) 1020°C-5min, (a, d) center area, (b, e) edge area.

4. Conclusions

(1) The PAG sizes show an inconspicuous effect on the quasistatic mechanical properties of hot stamping B1500HS steel. However, for hydrogen-charged samples, the loss of mechanical properties is exacerbated by decreasing PAG sizes.

(2) The impact of dislocation density on HE sensitivity is more significant than that of PAG size. The trapping effect of grain boundaries which impedes the hydrogen diffusion and leads to localized hydrogen accumulation.

(3) HMT results showed that hydrogen segregation occurs near the charging surface, especially with high dislocation density and finer PAG sizes. This local high hydrogen concentration promotes premature crack formation and increases HE sensitivity.

Acknowledgments

This work was supported by the National Key Research and Development Program of China (No. 2023YFB25046042, 2022YFE0196600), the National Natural Science Foundation of China (No. 52175349), and the Natural Science Foundation of Shanghai (No. 21ZR1429600).

Reference

1. H. Yu, A. Díaz, X. Lu, B. Sun, Y. Ding, M. Koyama, J. He, X. Zhou, A. Oudriss, X. Feugas, Z. Zhang, Hydrogen Embrittlement as a Conspicuous Material Challenge—Comprehensive Review and Future Directions, *Chem. Rev* **124** 6271 (2024).
2. M. Masoumi, L.P.M. Santos, I.N. Bastos, S.S.M. Tavares, M.J.G. da Silva, H.F.G. de Abreu, Texture and grain boundary study in high strength Fe–18Ni–Co steel related to hydrogen embrittlement, *Mater. Des.* **91** 90 (2016).
3. R. Latypova, O. Seppälä, T. Tun Nyo, T. Kauppi, S. Mehtonen, H. Hänninen, J. Kömi, S. Pallaspuuro, Influence of prior austenite grain structure on hydrogen-induced fracture in as-quenched martensitic steels, *Eng Fract Mech* **281** 109090 (2023).
4. Y. Liu, J. Lian, X. Han, Y. Yang, H. Yuan, Hydrogen embrittlement studies of hot-stamped boron steel with different prior austenite grain sizes, *J. Mater. Sci.* **58** 18187 (2023).
5. S.M. Teus, V.F. Mazanko, J.M. Olive, V.G. Gavriliuk, Grain boundary migration of substitutional and interstitial atoms in α -iron, *Acta Mater.* **69** 105 (2014).
6. R. Nazarov, T. Hickel, J. Neugebauer, First-principles study of the thermodynamics of hydrogen-vacancy interaction in fcc iron, *Phys. Rev. B* **82** 224104 (2010).

Open Access This chapter is licensed under the terms of the Creative Commons Attribution-NonCommercial 4.0 International License (<http://creativecommons.org/licenses/by-nc/4.0/>), which permits any noncommercial use, sharing, adaptation, distribution and reproduction in any medium or format, as long as you give appropriate credit to the original author(s) and the source, provide a link to the Creative Commons license and indicate if changes were made.

The images or other third party material in this chapter are included in the chapter's Creative Commons license, unless indicated otherwise in a credit line to the material. If material is not included in the chapter's Creative Commons license and your intended use is not permitted by statutory regulation or exceeds the permitted use, you will need to obtain permission directly from the copyright holder.

